CASL-U-2013-0093-000

Power uprates
and plant life extension

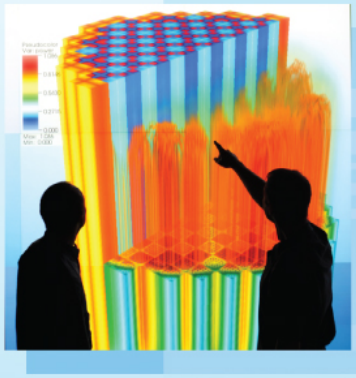

Engineering design
and analysis

Science-enabling
high performance
computing

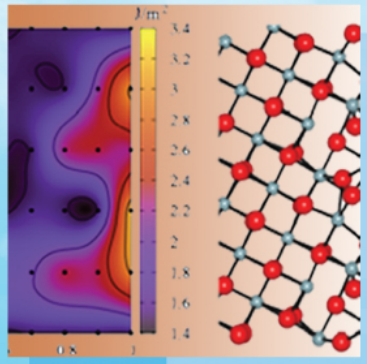

Fundamental science

Plant operational data

Consortium for Advanced Simulation of LWRs

Highly Resolved LES of Turbulent Convective Flow along a PWR Rod Bundle

MIT

D Cazviel, C Narayanan, D Lakehal

May 12-17, 2013:

U.S. DEPARTMENT OF ENERGY | Nuclear Energy

HIGHLY-RESOLVED LES OF TURBULENT CONVECTIVE FLOW ALONG A PWR ROD BUNDLE

D. Caviezel[1], C. Narayanan[1] and D. Lakehal[1,2]
[1] ASCOMP GmbH, Zurich Switzerland
[2] Nuclear Engineering Department, MIT, Cambridge USA

caviezel@ascomp.ch; lakehal@ascomp.ch (dlakehal@mit.edu)

ABSTRACT

A detailed numerical analysis of the turbulent convective flow along the heated rods of an idealized PWR sub-channel is investigated. The key predicted quantity is the length at which the rod surface temperature reaches nucleation temperature, approximated here as the saturation temperature. The turbulent effects are modeled using LES with very high grid resolution (~6 million cells) allowing resolving the viscous-affected layer. In a second step, boiling nucleation is triggered artificially and vapor bubbles are allowed to interact with the turbulent flow. We'll thoroughly discuss the results, including comparing the turbulence data basis with single-phase flow conditions.

1. INTRODUCTION

The onset of nucleate boiling on solid wall occurs when the temperature of the wall slightly exceeds saturation (Collier and Thome, 1996). The small vapor bubbles form and stay attached to the solid wall. Past the point of net vapour generation, the bubbles detach and remain trapped within a layer relatively close to the wall, beyond which – towards the core flow - they condense. Under turbulent conditions, the flow will be further affected by large and small eddies, affecting in turn the rate of wall-to-core-flow heat transfer and thus phase change, both near the wall (boiling) and far in the core flow (condensation). The first objective of this exercise is to assess the performance of the ITM/CFD code TransAT in predicting the turbulent convective flow upward along the heated rods of a PWR sub-channel. The key predicted quantity is the length at which the rod surface temperature reaches nucleation temperature, approximated here as the saturation temperature. For simplicity, we refer to it as the distance to the onset of nucleate boiling, or X_{ONB}.

Predicting this quantity correctly requires accurate prediction of turbulent flow, since the wall temperature is strongly dependent on the flow structures, its unsteadiness and stresses anisotropy. The problem is inspired by the PSBT OECD single sub-channel benchmark (Rubin et al., 2010), in terms of radial dimensions in particular, albeit the deliverables are different from the actual OECD case, in that the focus here is on detailed flow profiles and temperature at the wall rather than on global parameters as required in the benchmark. The operating conditions selected here are made on purpose different from PSBT, namely the power, which has been adjusted according to the reduced length (1m instead of 3.65m). The second objective is to provide a rich data basis to help assess the predictive performance of RANS turbulence models to predict mean and RMS profiles, stresses and turbulent fluxes, wall temperature at which saturation conditions are reached. In a second step the model is extended to two-phase flow with phase-change. We first

proceed by presenting the new approach for simulating the flow with LES in a rod bundle, supported by a thorough discussion of the results.

2. MODELLING

This work used one CFD code TransAT© developed at ASCOMP Switzerland, which is a multi-scale, multi-physics, conservative finite-volume solver for single- and multi-fluid Navier-Stokes equations. The grid arrangement is collocated, and the solver is pressure based (Projection Type), corrected via density for compressible flows. High-order schemes are employed; up to 3rd-order schemes in space and 5th-order in time (Runge-Kutta). Turbulent flows can be treated in two ways: RANS statistical models and Scale Resolving Approaches like LES and its DES and V-LES variants. LES is built within an explicit version, with specific routines for pressure coupling, boundary conditions, diffusive fluxes and near-wall stress integration. The schemes employed for pressure-velocity coupling include: GMRES, GMG & AMG, from the PETSc solver library. In LES the motion of the supergrid turbulent eddies is directly captured, whereas the effect of the smaller scale eddies is modelled or represented statistically by means of simple models, very much the same way as in Reynolds-averaged models (RANS); i.e. the usual practice is to model the sub-grid stress tensor by an eddy viscosity model. In terms of computational cost, LES (Sagaut, 2005) lies between RANS and DNS and is motivated by the limitations of each of these approaches. Since the large-scale unsteady motions are represented explicitly, LES is more accurate and reliable than RANS.

3. PROBLEM DESCRIPTION

The problem is inspired by the PSBT OECD sub-channel benchmark (Rubin et al., 2010) in terms of radial dimensions, though the expected deliverables are different, in that the focus is on detailed flow and temperature profiles in the subchannel, together with global parameters including the heat transfer coefficient, the onset of nucleation, the pressure drop and the thermal entry length (some only were required in the OECD benchmark). The operating conditions of the present case are made on purpose different from PSBT, namely the power and mass flow rate, which have been adjusted according to the reduced length (1m instead of 3.65m). The PWR fuel assembly consists of a rod bundle with water coolant flowing upward along the rods at a high Reynolds number. The rod diameter is 9.5mm, the rod pitch is 12.6mm and the active fuel length is typically ~3.7m. The hydraulic diameter for a unit cell is De=11.8mm. The coolant pressure is 15.5MPa with temperature ranging from 290°C to 340°C. Representative values of fluid properties are density: ρ=710 kg/m^3; surface tension: σ=0.0048N/m; dynamic viscosity: μ=9×10-5 Pa·s; thermal conductivity: κ=0.54W/m-K; heat capacity: Cp =5.9kJ/kg-K. The mass flux is G~3700 kg/m^{2}s, corresponding to a Reynolds number Re=GDe/μ~4.8×10^5, shear velocity u_τ ~0.2m/s, and frictional Reynolds number Re_τ ~10^4.

Several simplifications were adopted: First, the temperature of nucleation is assumed to be equal to the saturation temperature; second, a configuration consisting of the flow along a single sub-channel with periodic conditions is assumed; third, since the shear Reynolds number for the PWR channel is Re_τ~10^4, performing DNS for such flow conditions will be computationally prohibitive. As such, the problem has been scaled down to more reasonable conditions, i.e. $Re_\tau = 300$. Choosing LES instead of DNS is motivated by the fact that this problem should involve BFC meshing, which could introduce numerical diffusion for DNS. Finally, the length of

the domain was reduced from the PWR case to relax the meshing requirements in the axial direction. Since the distance to the onset of nucleate boiling depends on the integrated power supplied to the fluid, the heat flux was scaled accordingly. The PSBT operating conditions are summarized in Table 1. The imposed shear Reynolds number is Re_τ=300. Fluid properties assumed independent of temperature and are the same as in the actual case. The heat flux is to be applied at the rod outer surface. The actual operating conditions are summarized in Table 2.

Table 1 - Reference operating conditions for PSBT tests (Rubin *et al.,* 2010).

Pressure	15.5 MPa
Saturation temperature	344.6°C
Inlet temperature	290°C
Mass flux	3333 kg/m^{2}s
Heat Flux	581 kW/m^2
Power	2.7 MW

Table 2 - Test case 2 operating flow conditions.

Pressure	15.5 MPa
Saturation temperature	344.6°C
Inlet temperature	290°C
Mass flux	74.1 kg/m^{2}s (or Re_τ=300)
Heat Flux	50 kW/m^2
Power	1.57 kW

4. PROBLEM SETUP

4.1 Computational domain, boundary conditions & mesh

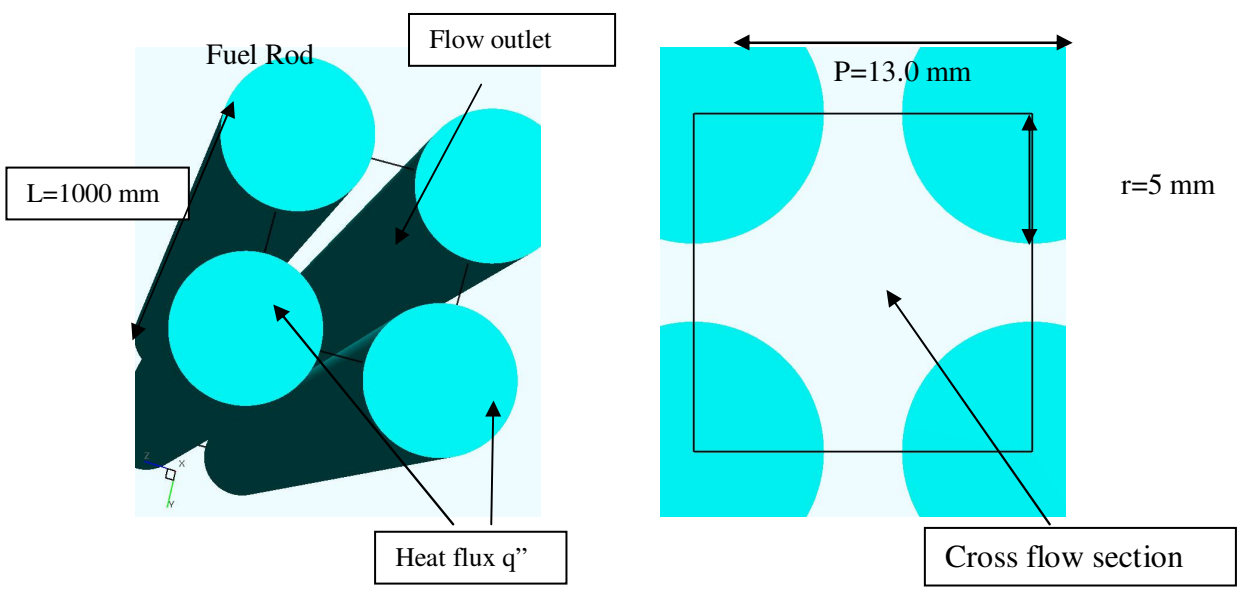

Figure 1 - Computational domain: Dimensions & BC's.

The dimensions of the simulation domain and boundary conditions are indicated in Figure 1. The case feature cross-sectional dimensions similar to the PSBT OECD case; rod diameter D = 10 mm and pitch P = 13 mm. The length is reduced from 3.6 m to 1.0 m. A novel approach was used to generate proper boundary conditions for this flow. First, periodic conditions were applied in the radial and circumferential directions to mimic the effect of the neighbouring rods. In the axial direction, however, a hybrid 'Developed & Developing Flow Hybrid Approach' has been developed. It consists of first generating turbulence in a periodic domain of length 2πDe, then the resulting fluctuating (scaled to maintain the mass flow rate) field is imposed in the entire domain, recycled periodically: temperature is updated using inflow-outflow BC's, together with the steam-water interface in case of two-phase flow calculations. Two BFC grids were employed (Table 3): the medium one consists of 798×40×40 cells providing a near-wall resolution of y^+~0.5-2.1, which allows resolving the viscous sublayer. The second grid consists of 1,600x60x60 cells, providing a near-wall resolution of y^+~0.4-1.5.

Table 3 - Grid properties used for Test Case 2.

Re_τ=300	**Number of nodes**		**Resolution**		**Grid type**	**total number of cells**
	x-y	*z*	Δx^+-Δy^+	N blocks		
Grid Med	40-40	798	0.5-2.1	208	BFC	**1,317,400**
Grid Fine	60-60	1600	0.4-1.5	832	BFC	**6,011,200**

4.2 Initial conditions

The initial flow conditions for the full domain were generated from an earlier flow solution obtained using cyclic inflow-outflow in a shorter 2πDe long domain. During this process, to speed up the turbulent flow generation, various grids of different refinements (coarse, medium and refined) were employed in a sequential way: the solution obtained on the coarse grid is mapped into the medium one, the solution of which is then passed to the fine mesh, which at the end is transferred to the final run as an initial/inflow/outflow condition. Assuming the flow to be non-homogenous with a dominant velocity fluctuation in the flow direction, component w' (in the flow direction) fixed as the variance of u_τ. The other components were defined as u'=2/3w' and w'=1/3u'. This process is innovative; it allows generating the fluctuating field to the finest mesh (56x56 in cross section) rather fast.

4.2 Simulations parameters

The simulations were performed on DOE's supercomputer Jaguar, using 144 and 832 MPI cores for the medium and fine grids, respectively. The DSM model presented earlier was used for LES. In the medium grid, flow averaging started at 20,000 time steps, with 80,000 additional steps to infer ergodic conditions, for achieving around 6 flow-through times. In the fine grid, averaging started at 28,450 iterations extending for a total of 262,000 time steps, for achieving around 8 flow-through times. Overall it took more than six weeks to get the 262,000 time steps of fine-grid simulation performed and time averaged. The most important indicator of turbulence being developed is the wall shear velocity; u_τ, which converged to 0.0065 m/s for the fine grid and to 0.0064 m/s for the medium one.

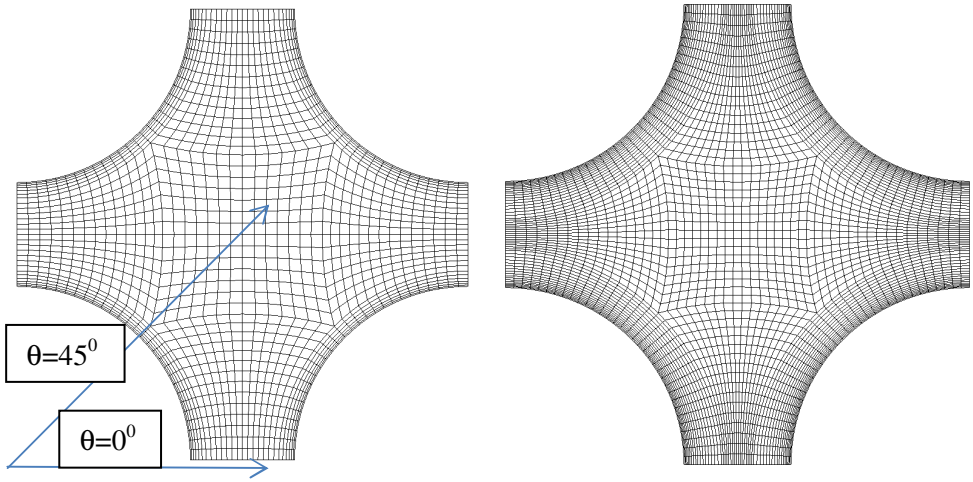

Figure 2 - Medium (left) and fine (right) grids for LES (x-y). Arrows show 0^0 and 45^0 segments.

5. SIMULATION RESULTS

5.1 Flow structures results

The flow structure at various instances near the central area obtained for the medium and the fine grids are compared in Figures 3 and 4. While no major differences can be observed, the cross-sectional views show more structures developing in the fine grid simulation (upper panel), as was to be expected. Temperature contours on the rod surface show intermittent patches related to turbulence eddies transporting heat from the wall to the core flow. Secondary flow motion is quite strong. Instantaneous and time averaged results are depicted in Figures 5 and 6. Important point to note is that the final mean flow exhibits in both grid simulations a secondary flow motion (intensity not to scale). The effect of this secondary cross-flow motion is on the wall temperature, showing a patchy structure due to turbulent, intermittent wall streaks. This is clearly indicated by the time averaged temperature contours plotted in Figure 6, indicating the position for saturation temperature (618°K) marked by a black line. In both medium and fine-grid simulations, the line varies spatially by about 5-7% around the mean values.

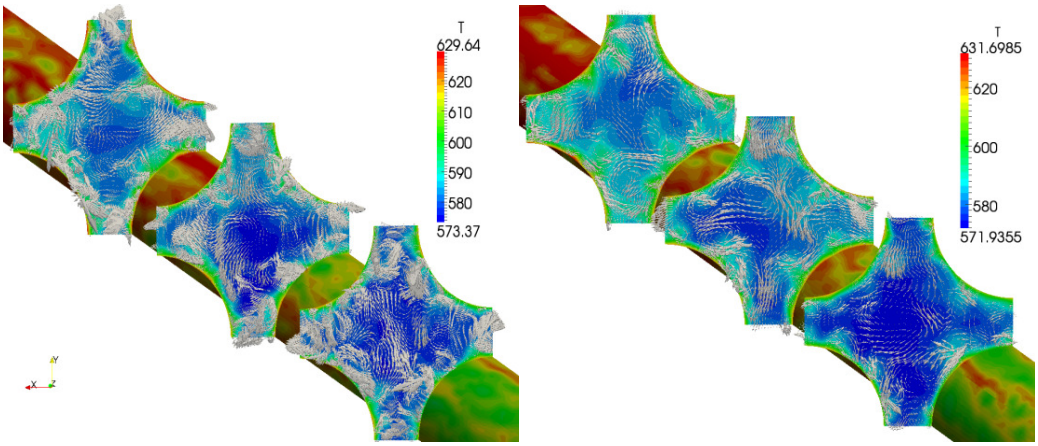

Figure 3 - Fine (left) vs. medium (right) grid: Instantaneous velocities and temperature contours.

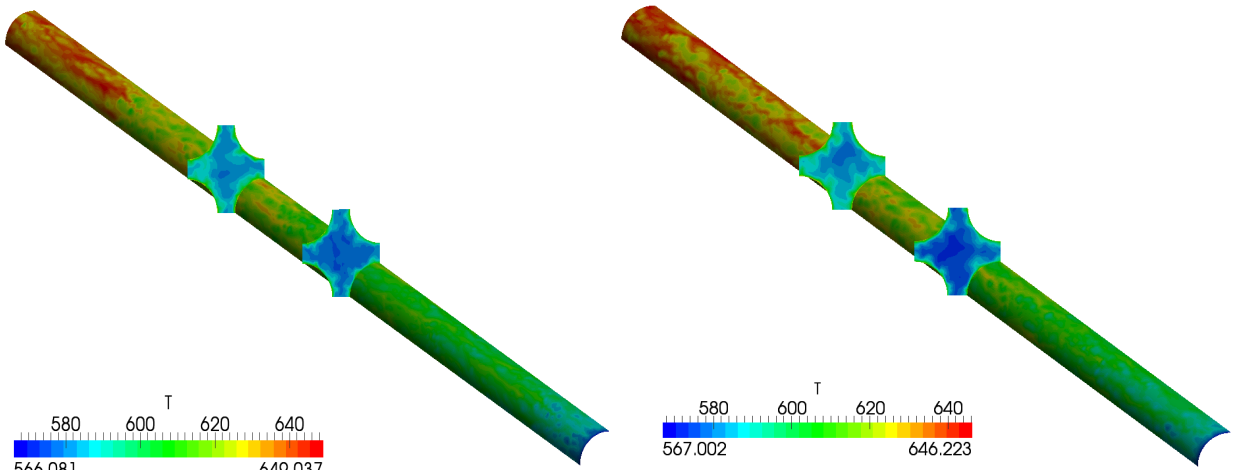

Figure 4 - Fine (left) vs. medium (right) grid: Instant cross-sectional velocities and temperature contours.

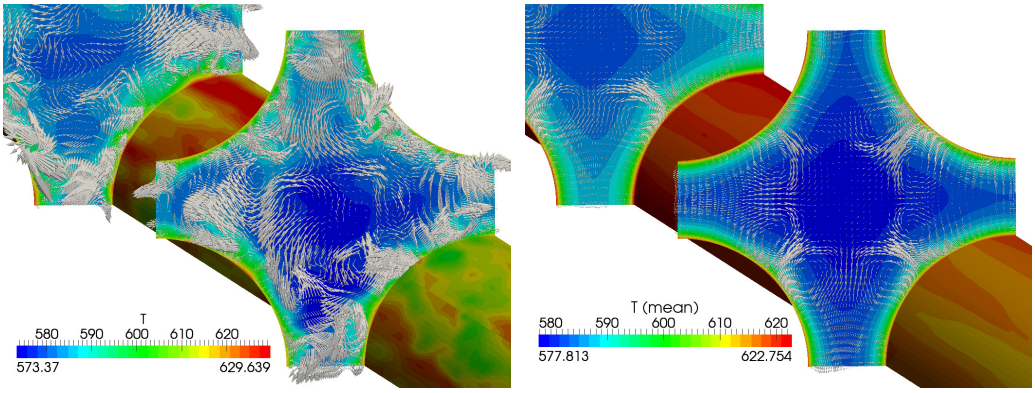

a) Fine grid: instantaneous b) Fine grid: time average

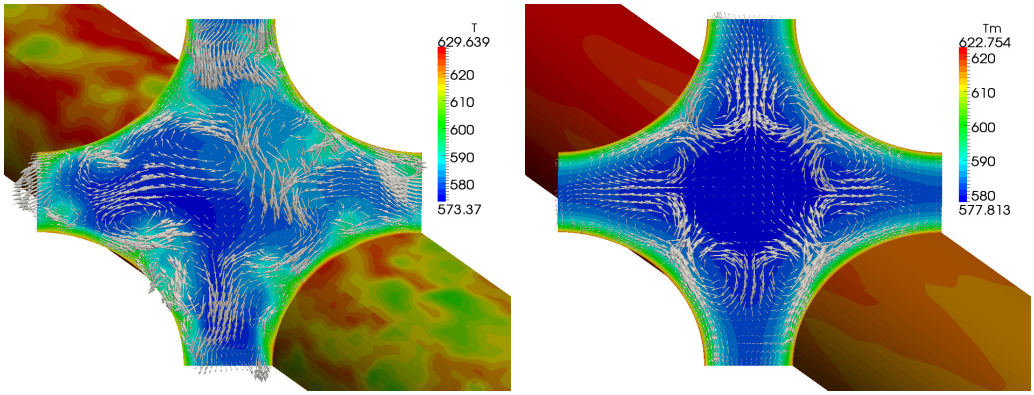

c) Medium grid: instantaneous d) Medium grid: time average

Figure 5 - Fine vs. medium resolutions: Instantaneous (a and c) and time averaged (b and d) cross-sectional velocities and temperature contours.

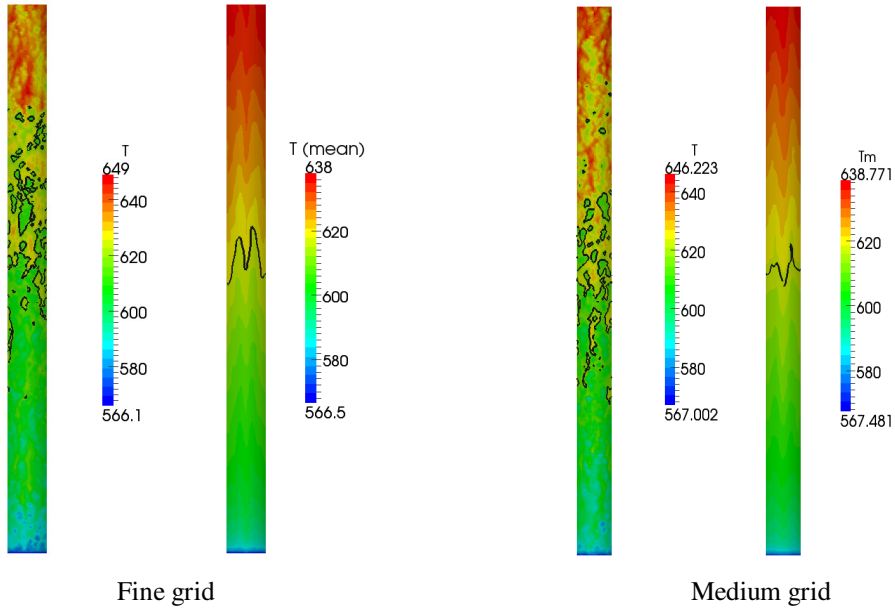

Figure 7 - Fine vs. medium resolutions (scaled domain for illustration): Instantaneous and time averaged temperature contours. The black line on the right panel indicates X_{onb}, the position of $T_{sat.}$

5.2 Time averaged results

Time averaged results are presented in Figures 8 through 12, including flow and temperature mean and turbulent profiles. Since the flow resembles turbulent flow in a pipe, use was made of available DNS data at Re_τ=360 (Eggels, 1994) for comparison. The DNS data are not filtered. The difference with the pipe flow is that the present one has two azimuthal segments, a short one ($\theta=0^0$) with low Re effects and a full one ($\theta=45^0$) extending to the core with high Re effects (see Figure 2); the latter one should thus return the imposed shear Reynolds number at the subchannel center point, in the form of $y^+|_{centerline}= Re_\tau$.

The mean flow profiles are plotted in Figure 8, compared to DNS. As explained earlier, the $\theta=0^0$ segment profile achieves a lower y+ than the $\theta=45^0$ one. The profiles match very well the DNS data of Eggels (1994), in particular the fine grid one which does not show the slight grid effect returned by the medium grid simulation. This preliminary important result pleads in favour of a high quality LES simulation achieved by TransAT. Figure 9 compares the medium and fine mesh simulations data for the mean temperature profiles across the subchannel at various streamwise locations (0.25L to 0.95L). The comparison reveals that the deviations between the two sets of grids are really minimal. The thermal boundary layer profiles develop overall at about 0.3R. The profiles show a different near-wall behaviour in the $\theta=45^0$ segment, or more precisely a very good near-wall resolution of the thermal boundary layer.

Another important measure is the normalized temperature variance $< \theta'\theta' >$, which is plotted in Figure 10 on both segments, at various cross-flow locations, comparing once more the medium and fine grid results.

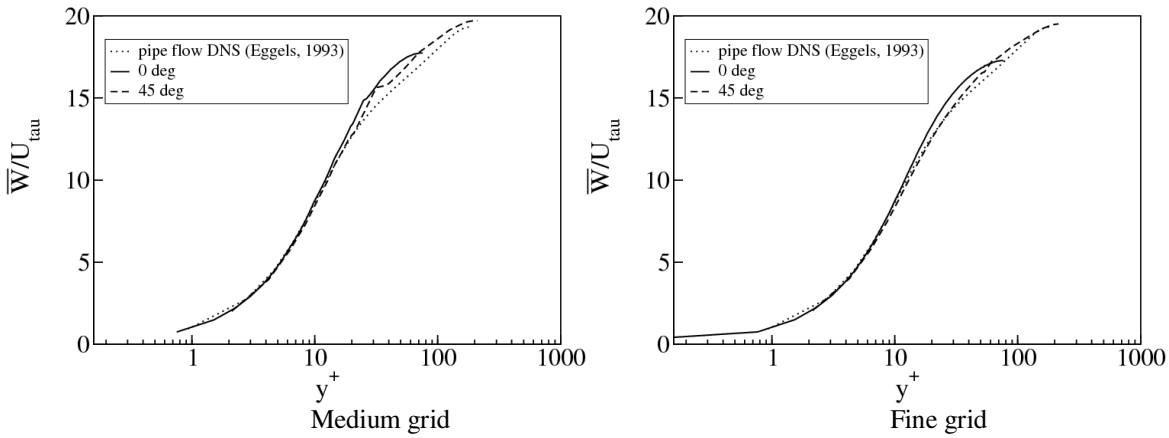

Figure 8 - Mean velocity profiles across the subchannel (0^0 & 45^0) compared to the DNS of Eggels (1994).

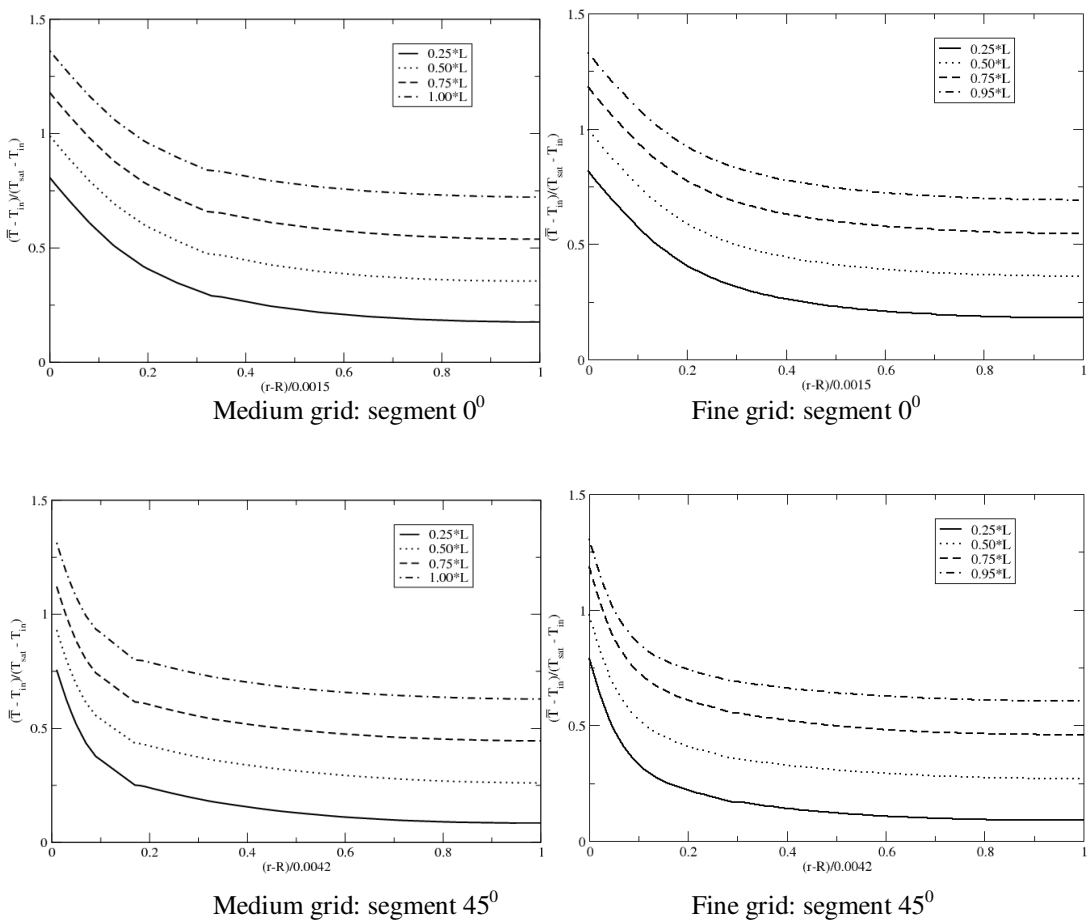

Figure 9 - Mean temperature profiles across the subchannel at various streamwise locations.

It is only for this higher-order quantity that the grid resolution shows an effect, with differences in peak values of about 5% in the $\theta=0^0$ segment and up to 10% in the $\theta=45^0$ one. The medium

grid results still show a grid effect (kink). The fine grid results exhibit variations in this quantity with elevation, which is not always the case in the medium grid results. This may be an artefact of normalization; it could have shown a self-similar behaviour if it were normalized by the average wall temperature. We also suspect that the fine grid simulations require still more time to reach statistical convergence, in particular for second-order turbulent quantities. Be it as it may, the results are similar to DNS data of a heated channel flow. Figure 11 compares the averaged flow-direction normal stresses (<w'w'>) profiles; medium vs. fine grid resolutions. The data are also compared to DNS of Unger & Friedrich (1993). Here again we plot the 00 low-Re segment and the 45^0 high-Re core-flow one. Note that it is difficult to extract the azimuthal profiles since the operation requires a space transformation operation of these stresses. This is true of the heat fluxes in the azimuthal directions as well. While the medium grid shows a slightly over-predicted normal-stress value in the core flow, the fine grid provides a very good match in terms of trend with DNS, although our case is a higher Re case compared to the DNS and as such it should return a higher r.m.s value. Figure 12 compares the time averaged heat flux (<w'θ'>) profiles. Small differences between the medium and fine grid results are to report. Otherwise the results look again similar to channel flow data (Lakehal et al, 2011). The convergence rate seems to be acceptable for these quantities.

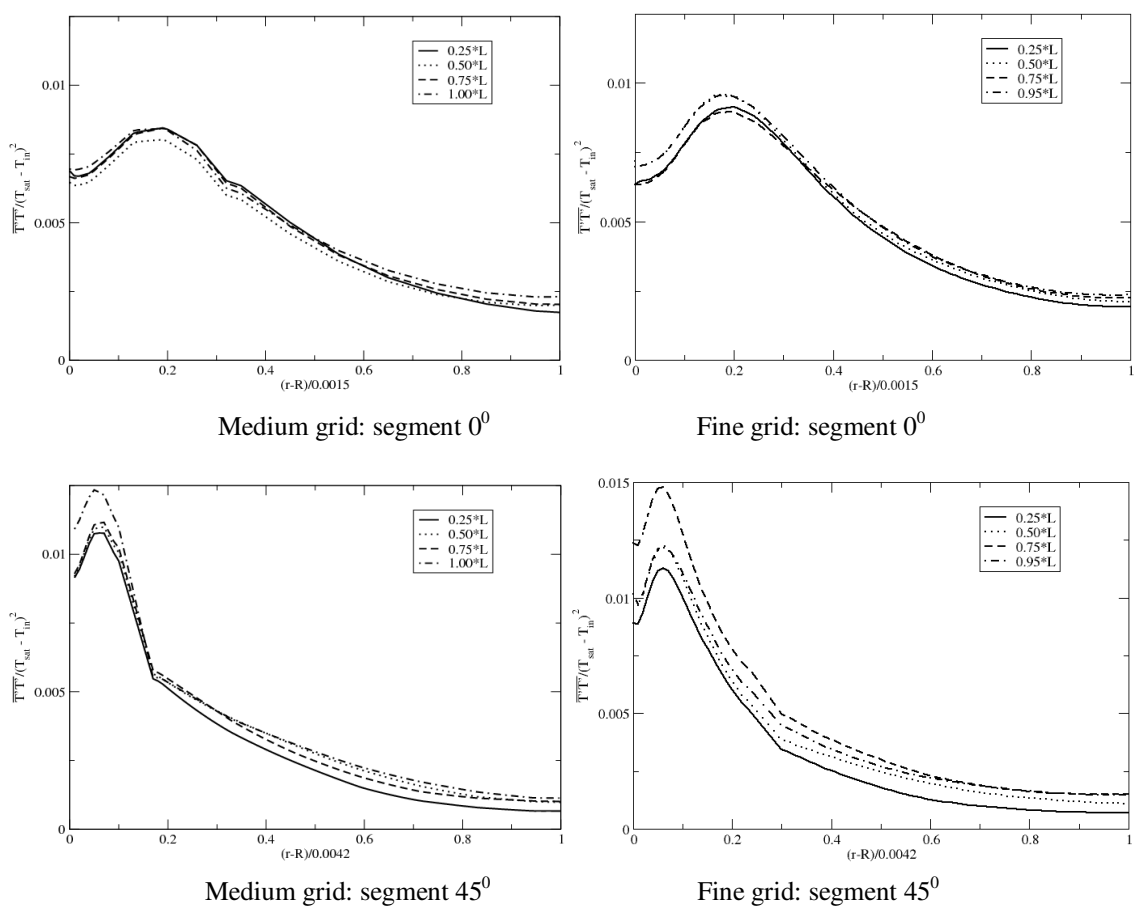

Figure 10 - Temperature variance profiles (<θ'θ'>) at various streamwise locations of the subchannel

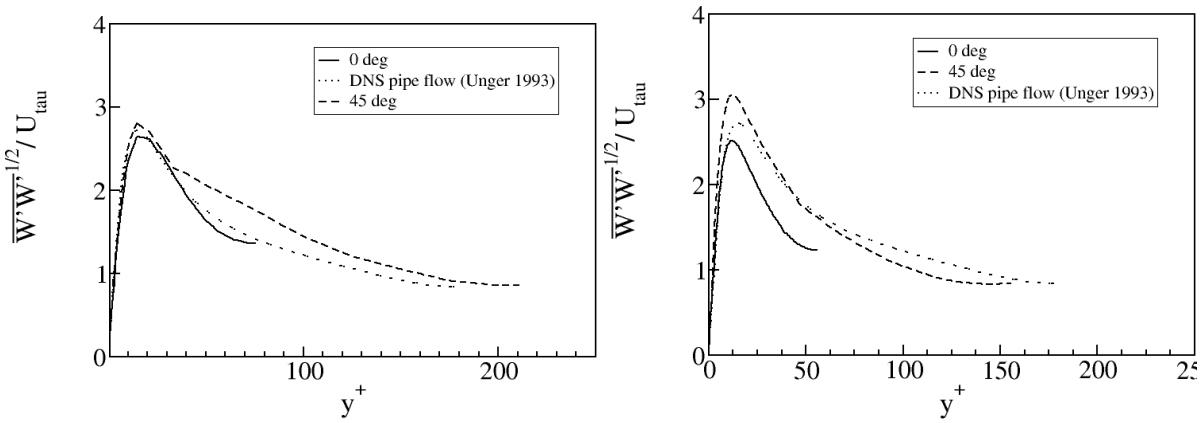

Figure 11 - Averaged normal-stresses profiles (<w'w'>)

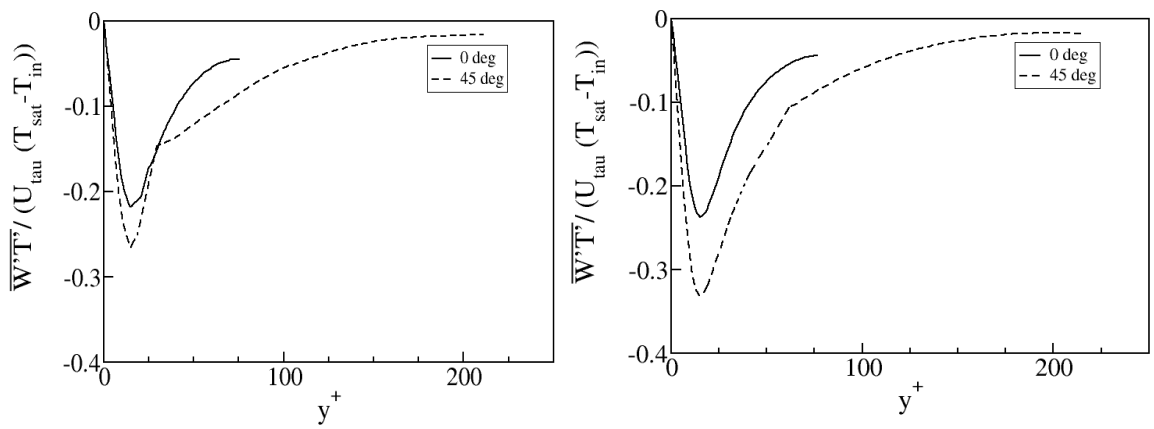

Figure 12 - Averaged heat flux profiles (<w'θ'>). Fine grid: 0^0 & 45^0

5.3 Global parameters results

Global parameters results are presented in Table 4. The LES results are compared here to existing analytical and experimental correlations. The pressure drop between medium and fine grid is accurate to 2.2% and 5% compared to the correlation. As to the heat transfer coefficient (HTC), there are uncertainties for the case of interest, which in fact belongs to the 'transitional cases regime', according to Incropera and DeWitt (1996), for which the correlations, in particular the Colburn one (or Dittus-Boelter), could give up to 25% error. When accounting further for the effect of neighbouring rods using the Weisman correction (here Ψ=1.826p/D-1.043=1.33), the deviations between LES and correlation is high, and is precisely 33%. If this correction is not accounted for, the LES results (fine grid in particular) are comparable to the Colburn correlation, within -5%. With more sophisticated correlations e.g. the Gnielinski and Petukov (see Incropera and DeWitt, 1996), the analysis changes, in that the LES data are 6% than Gnielinski's correlation and 1.9% only than Petukov's one. The distance to the onset of boiling is questionable in the same way, since it is directly based on the HTC correlation employed (here we took the Colburn one only). The simulation results are within a few percent's deviations from the Colburn correlation, but 24-35% off the Colburn–Weisman variant, which is in line with the HTC deviations reported. Finally, as stated previously, there is no such a constant line indicating

XONB since the simulations have clearly shown that the effect of the secondary flow motion makes it rather undulating by 5-7% around the mean.

Table 4 - Test case 2 operating flow conditions

Quantity	Med. grid	Fine grid	Analytical/Exp.
Pressure drop ΔP [Pa]	10.223	10.52	10.0
Heat transfer coefficient (HTC) at X_{ONB} [kW/m^{2}K]	1.495	1.535	1.62 (Colburn)
			2.16 (Colburn -W*)
			1.44 (Gnielinski)
			1.99 (Gnielinski -W)
			1.50 (Petukov)
			2.0 (Petukov -W)
Distance to X_{ONB} [m]	Min-max 0.49–0.57	Min-max 0.49–0.6	0.59 (Colburn)
			0.79 (Colburn -W)
Thermal entry length [m]	Min-max 0.21–0.28	Min-max 0.21–0.29	0.29–0.46

*W means with the Weisman (1959) correction factor

6. CONCLUSIONS

The paper reports a detailed LES-based analysis of turbulent convective flow upward along the heated rods of a PWR sub-channel using the code TransAT. The LES results have been compared to DNS data of pipe flow, which is quite similar to the present flow. The comparison with correlations as to engineering parameters show that excellent results are obtained for pressure drop, but raise important questions as to the validity of heat-transfer coefficient correlations in this transitional regime, and indirectly the location of onset of boiling. The data basis can be made available for use to address RANS models. The simulation campaign is being now extended to boiling heat transfer.

7. ACKNOWLEDGEMENTS

This work was financially supported by the US Department of Energy through the CASL project. The simulations were performed in the Jaguar supercomputer (ORNL). The authors would like to acknowledge the support of the MIT team: Prof. J. Buongiorno and Dr D. Chatzikiriakou.

8. REFERENCES

[1] J.G.M. Eggels et al., 1994. Fully developed turbulent pipe flow: A comparison between direct numerical simulation and experiment. J. Fluid Mech., vol. 268, pp. 175-209.

[2] H. Incropera, J. DeWitt, 1996. Intr. Heat Transfer, Wiley & Sons. Third Edt.

[3] D. Lakehal et al., 2011, Progress in the Prediction of Non-unity Pr Number Flows using TransAT, Proceedings of the 14th International Topical Meeting on Nuclear Reactor Thermal-Hydraulics (NURETH14), Toronto, Sep. 2011.

[4] A. Rubin et al., 2010. OECD/NRC Benchmark based on NUPEC PWR subchannel and Bundle Tests (PSBT), NEA/NSC/DOC(2010)1.

[5] P. Sagaut, 2005. Large Eddy Simulation for Incompressible Flows: An Introduction , Springer Pubs.

[6] P. Moin, K. Squires, W. Cabot, S. Lee, 1991. Phys. Fluids, 3(11), pp. 2746-2757